Precast concrete double-tee connectors, part 2: Shear behavior

Liling Cao and Clay Naito

Postearthquake reconnaissance following the 1994 Northridge, Calif., earthquake revealed that precast concrete parking structures were susceptible to damage of the floor diaphragm.[1] The unexpected response of these systems underscored a need for comprehensive reexamination of precast concrete floor diaphragms for seismic demands. To clarify current diaphragm design procedures and to develop a seismic-resistant precast concrete floor diaphragm, PCI and the National Science Foundation (NSF) funded a research program. The program, Development of a Seismic Design Methodology, was initiated by a collaboration of three university teams.[2,3] One of the initial steps of the research program was to characterize the performance of conventional diaphragm connectors.

Behavior of precast concrete floor diaphragm systems is one of the most complex and least understood aspects in current seismic design practice. Recent analytical studies have shown that diaphragm joints are subjected to complex shear, tension, and compression deformation demands during an earthquake.[4] To design precast concrete floor diaphragms for seismic demands, methods must be available for estimating the load capacity and deformability of local connections under a combination of in-plane demands.

To develop estimates of the strength and deformation capacity of diaphragm connections, a number of experimental studies were conducted. Published research began with hairpin connectors in 1968[5] and has continued to recent studies on a variety of mechanical connectors and proprietary connections.[6–14] Naito and Cao summarized a large portion of these studies.[15] That paper provides a comparison of the responses for connectors examined under both load and deformation demands. A review of past connection testing indicates that a limited group of connectors was examined. Most connectors were examined under in-plane shear, but few were examined under in-plane tension

Editor's quick points

- This is the second part of a two-part paper that discusses a research program to develop a seismic design methodology for precast concrete diaphragms. The program was partially funded by PCI.

- The research program categorizes the strength and deformation capacity of common double-tee web and chord connectors subjected to in-plane shear or tension loading.

- This paper presents recommendations on connector detailing to improve connection strength and deformability.
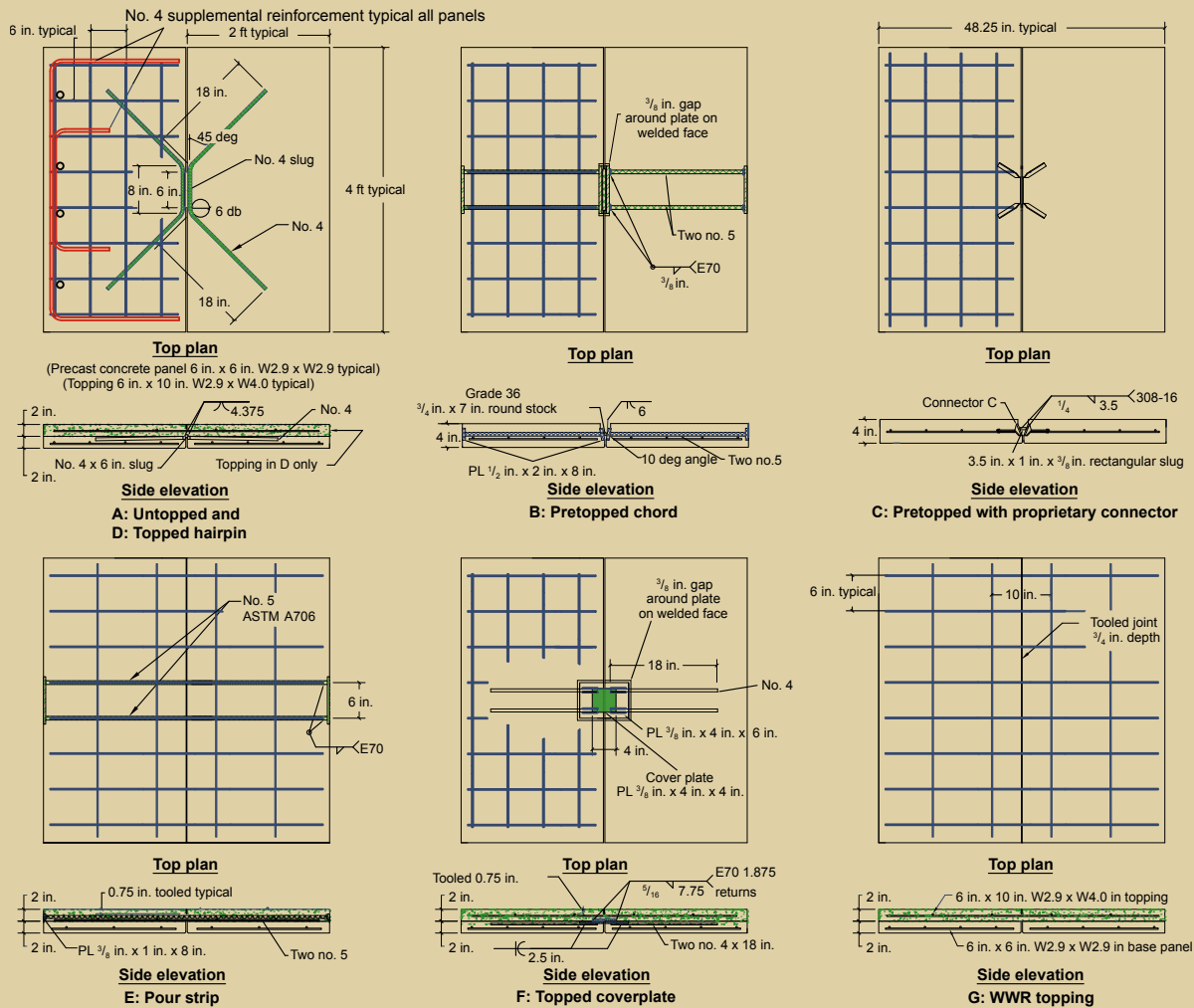
Figure 1. This plan view shows the connection specimens. Note: PL = plate; WWR = welded-wire reinforcement. No. 4 = 13M; no. 5 = 16M; 1 in. = 25.4 mm; 1 ft = 0.305 m.

as well. Furthermore, the method of evaluation used for each group of connectors varied based on the preference and capability of each research facility, rendering direct comparison of the results questionable.

Most studies have focused on the response of web connectors subjected to shear. Data on the shear response of chord connectors and the contribution of the topping to the connection strength have not been extensively investigated. Furthermore, a number of shear tests were performed on a single panel.[10,11,13] In these tests, shear demand was applied to the welded connector via a stiff loading beam. Under these conditions, the connector is artificially restrained transverse to the in-plane shear by the rigidity of the loading beam. This restraint produces an axial force on the connection, which in most cases was not monitored.

Test results indicated that the shear strength is sensitive to the axial force present on the connection. In 1998, research conducted by Pincheira et al.[9] examined the combined loading effect on the connection force and deformation

capacity by applying a load at an orientation of 45 deg to the joint. This load trajectory resulted in an equal amount of shear and tension force demand on the connector. The hairpin connector was found to decrease initial stiffness and ultimate strength under this force combination. While this test series provided valuable information on combined force demands on connectors, the study was limited to one force combination. Due to the physical construction of precast concrete floor diaphragms, the connectors are commonly subjected to a combination of in-plane shear and axial deformations as opposed to a prescribed combination of shear and axial forces. Furthermore, finite-element studies of floor diaphragms indicate that the combined shear and tension ratio could vary depending on the connection flexibility and its location in the diaphragm.[16]

To effectively examine the sensitivity of shear response to the axial demand, a group of web and chord connections in pretopped and topped systems was examined under in-plane shear and combinations of in-plane shear with tension deformation using a consistent experimental methodology.

Experimental program

Seven connection types (A through G) were selected from an industry survey to be examined as part of the experimental program (**Fig. 1**). The connections were developed in collaboration with an industry advisory board to model current detailing techniques. Each specimen represented a precast concrete double-tee connection commonly used for pretopped or topped diaphragm systems. A background discussion of each connection detail can be found in the first part of this two-part paper.[17]

Each connection was evaluated for both tension and shear capacity. The tension response was presented in part 1,[17] with either shear deformation or force maintained at zero or kept proportional to the tension demands. In this paper, the shear response is presented.

Shear deformation Δ_v was applied with tension deformation Δ_t held constant or kept proportional to the shear deformation with joint rotation prevented. The field-topped connections were precracked and held at a constant joint tensile opening of 0.1 in. (2.5 mm). This width of the opening was chosen to represent thermal and shrinkage effects commonly observed in parking structures. The pretopped connections were maintained with no joint opening.

To evaluate the sensitivity of shear capacity to concurrent tension, the connectors were subjected to combined shear with tensile deformation demand. A pushover analysis of a diaphragm reinforced with conventional connectors revealed that common shear-to-tension deformation ratios are generated at different joint locations within the diaphragm.[16] In the elastic range of diaphragm response, a shear-to-tension deformation ratio of 2.0 is expected for connections located close to lateral-force-resisting boundary elements, while a shear-to-tension ratio of 0.5 is expected for chord connections adjacent to the midspan.

A multidirectional test fixture was used for simultaneous control of shear, axial, and bending deformations at the panel joint while providing continuous measurement of the forces generated or resisted. The fixture used three actuators: two in axial displacement and one in shear displacement (**Fig. 2**). Independent control of the three actuators allowed for application of proportional or nonproportional combinations of shear and tension or compression deformation on the connection.

Tests were conducted under displacement control at quasi-static rates (<0.05 in./sec [1.3 mm/sec]). All specimens were displaced until the force capacity approached zero. Both monotonic and cyclic displacement protocols were used (**Fig. 3**). The cyclic protocol consisted of three cycles at increasing levels of shear displacement. Four elastic displacement levels were applied. The inelastic levels increased at a rate in accordance with a protocol developed for the PRESSS (Precast Seismic Structural Systems) program.[18]

In-plane shear performance

To examine the in-plane shear resistance of the connections, a variety of loading protocols were applied (**Table 1**). The protocols chosen for each connection were based on the primary usage of the connection in resisting diaphragm forces. Pretopped details—including the hairpin A, stud-weld connector B, and proprietary connection C—were subjected to monotonic shear (MV) and cyclic shear (CV) without tensile opening, and a combined monotonic shear with tension (MVT). Topped connections—including topped hairpin D, topped chord E, and cover plate F connections—were subjected to monotonic and cyclic shear with a constant tensile opening of 0.1 in. (2.5 mm) and a combined monotonic shear with tension. The opening of 0.1 in. was chosen to represent a precracked condition of the joint.
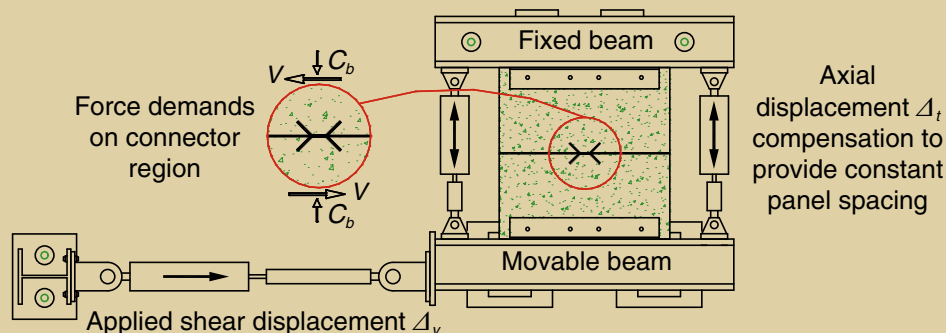

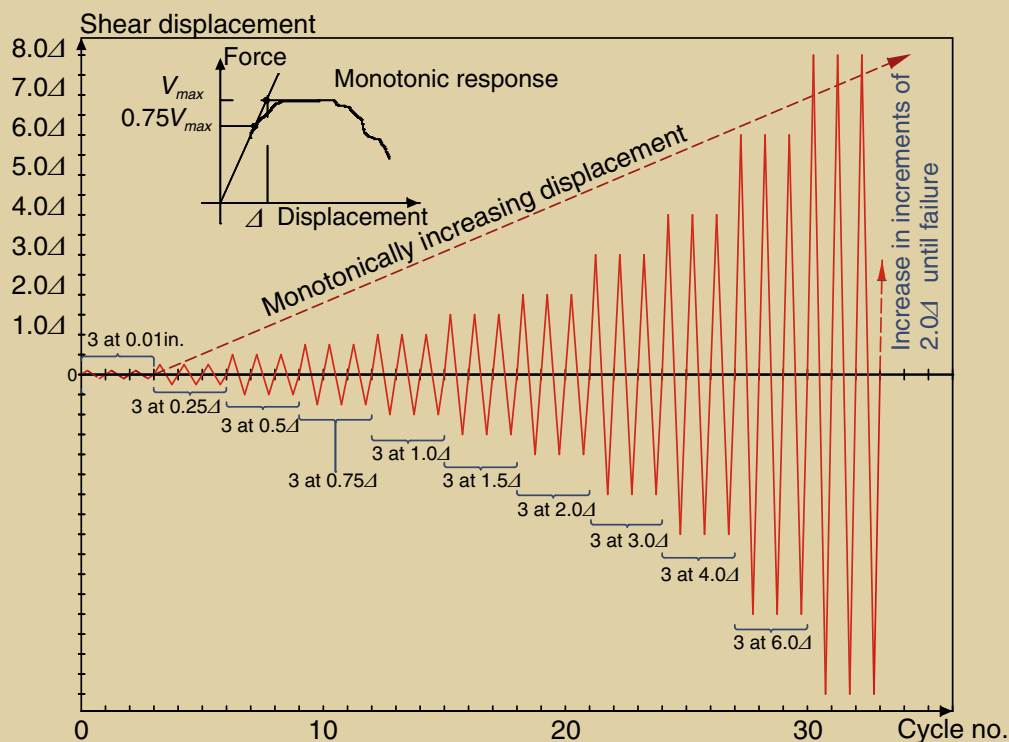**Figure 2.** This drawing illustrates the shear test setup.

Figure 3. Both monotonic and cyclic displacement protocols were used during testing. Note: Δ = yield deformation from monotonic test. 1 in. = 25.4 mm.

Based on the diaphragm analysis, a proportional shear-to-tension deformation ratio Δ_v/Δ_t of 0.5 was applied to the chord connection E, and a ratio of 2.0 was applied to the web connectors A, B, C, D, and F for the combined loading test (MVT). The topping connection G with welded-wire reinforcement (WWR) was examined under monotonic shear with 0.1 in. (2.5 mm) tensile opening, and monotonic and cyclic shear without tensile opening.

Table 1 summarizes the measured performance of seven connections. A four-point, simplified backbone curve in accordance with Federal Emergency Management Agency[19] recommendations was developed for each test (**Fig. 4**). Point *a* is defined as occurrence of yield. For connections without a clearly defined yield point, point *a* is defined as the point where the shear strength achieves 75% of peak resistance. Initial shear stiffness was calculated as the secant of strength-displacement relationship from origin to point *a*. Point *b* represents the peak load and point *c* is defined as the failure level. The points are defined in terms of the shear resistance values V_a, V_b, and V_c and the corresponding displacements ΔV_a, ΔV_b, and ΔV_c. In addition, Table 1 presents the coupled axial force at the level of peak shear resistance C_b. The positive force of C_b refers to the tension that opens the joint, and negative force is the compression that closes the joint. The shear stiffness K_s is the secant at point *b*. The measured shear resistance divided by the estimated strength V_{es} is tabulated for comparison. The

formulations used for the estimated strengths are presented in the section "Shear Design Strength."

Experimental results

The connections exhibited a wide range of shear resistance and deformation capacities. **Figure 5** summarizes the monotonic shear, shear with tension, and cyclic shear response of each connection. Connections A and C exhibited flexible and ductile shear responses, while connections B, D, E, F, and the uncracked topping G initially exhibited a stiff response with either minimal or no yield plateau. The majority of connections that were examined exhibited brittle concrete crushing and spalling followed by connector fracture. The pretopped and topped chords (B and E), however, did not fracture and were capable of sustaining large deformations. **Table 2** presents the photos of each specimen at the end of the test.

Experiment observations

The connections resisted shear through bearing of the connector's front face and anchorage of the bars in the concrete. Thus, characteristics of the shear response depended on concrete spalling, cracking, and crushing modes of failure that occurred under these bearing modes. For the untopped hairpin connection A, embedment of the front face was minimal because the bar was angled into

Table 1. Test results

Connector ID	Test type	Point a			Point b			Point c		V_b/V_{es}
		K_s, kip/in.	ΔV_a, in.	V_a, kip	ΔV_b, in.	V_b, kip	C_b, kip	ΔV_c, in.	V_c, kip	
A	MV ($\Delta_t = 0$)	67.5	0.07	4.585	1.282	8.66	4.54	1.764	2.245	0.931
B	MV ($\Delta_t = 0$)	514	0.083	42.67	0.131	56.90	-49.86	>0.900	10.37	1.942
	MVT ($\Delta_v/\Delta_t = 2$)	225	0.117	26.18	0.270	34.91	9.66	0.890	12.13	1.191
	CV ($\Delta_t = 0$)	373	0.117	43.6	0.238	56.30	-37.50	0.638	4.10	1.922
C	MV ($\Delta_t = 0$)	162	0.062	10.07	0.767	35.87	-24.00	1.494	16.12	2.085
	MVT ($\Delta_v/\Delta_t = 2$)	170	0.122	20.55	0.209	27.40	-5.50	1.441	24.51	1.593
D	MV ($\Delta_t = 0.1$)	210	0.197	41.20	0.342	54.90	-24.50	2.828	20.00	1.806
	MVT ($\Delta_v/\Delta_t = 2$)	257	0.087	22.35	0.201	29.80	20.50	0.550	20.94	0.980
	CV ($\Delta_t = 0.1$)	210	0.167	35.2	0.254	42.50	-14.50	0.636	13.7	1.398
E	MV ($\Delta_t = 0.1$)	210	0.123	25.35	0.365	33.80	20.00	>3.500	9.00	0.913
	MVT ($\Delta_v/\Delta_t = 1/2$)	260	0.027	7.05	0.040	9.40	52.00	1.075	4.80	0.254
	CV ($\Delta_t = 0.1$)	205	0.047	9.50	0.094	11.20	40.00	>2.600	3.50	0.303
F	MV ($\Delta_t = 0.1$)	197	0.205	40.42	0.338	53.89	-31.47	2.290	15.43	1.953
	MVT ($\Delta_v/\Delta_t = 2$)	240	0.107	25.60	0.179	34.12	11.25	0.896	6.52	1.236
	CV ($\Delta_t = 0.1$)	170	0.066	11.25	0.088	15.00	20.00	0.645	1.70	0.543
G	MV ($\Delta_t = 0.1$)	35	0.234	8.25	0.372	11.00	13.01	0.500	2.50	0.932
	MV ($\Delta_t = 0$)	338	0.089	30.05	0.227	40.07	-37.40	1.500	7.70	1.452
	CV ($\Delta_t = 0$)	260	0.029	7.50	0.054	10.20	-7.50	0.454	1.60	0.370

Note: CV = cyclic shear; MV = monotonic shear; MVT = combined monotonic shear with tension. C_b = coupled axial force at the level of peak shear resistance; K_s = shear stiffness; V_a = shear resistance at point a; V_b = shear resistance at point b; V_c = shear resistance at point c; V_{es} = estimated strength; Δ_t = tension deformation; Δ_v = shear deformation; ΔV_a = shear displacement at point a; ΔV_b = shear displacement at point b; ΔV_c = shear displacement at point c. 1 in. = 25.4 mm; 1 kip = 4.448 kN.

the panel from the top at the face of the panel to mid-depth at the end of the legs. This resulted in limited bearing and a low level of resistance but a large deformation capacity. Connection B, however, consisted of a faceplate anchored in the mid-depth of the panel. This faceplate provided a significant bearing area, resulting in a stiff but brittle response. The sensitivity of response to the bearing area was common to all connections:

- Hairpin connection A exhibited bending of the compression leg and concrete spalling at the tension leg. This allowed rotation of the slug-connector region over 0.1 in. to 0.5 in. (2.5 mm to 12.7 mm) of shear deformation. After this point, the rotation was large enough to transfer shear through axial deformation of diagonally opposing tension legs, resulting in an increase in load-carrying capacity. Spalling propagat-
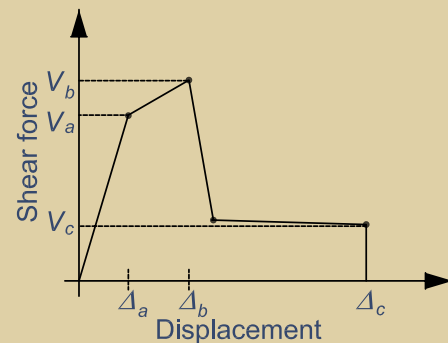

Figure 4. A simplified response curve was developed for each test in accordance with recommendations in Federal Emergency Management Association 273, *NEHRP Guidelines for the Seismic Rehabilitation of Buildings.*
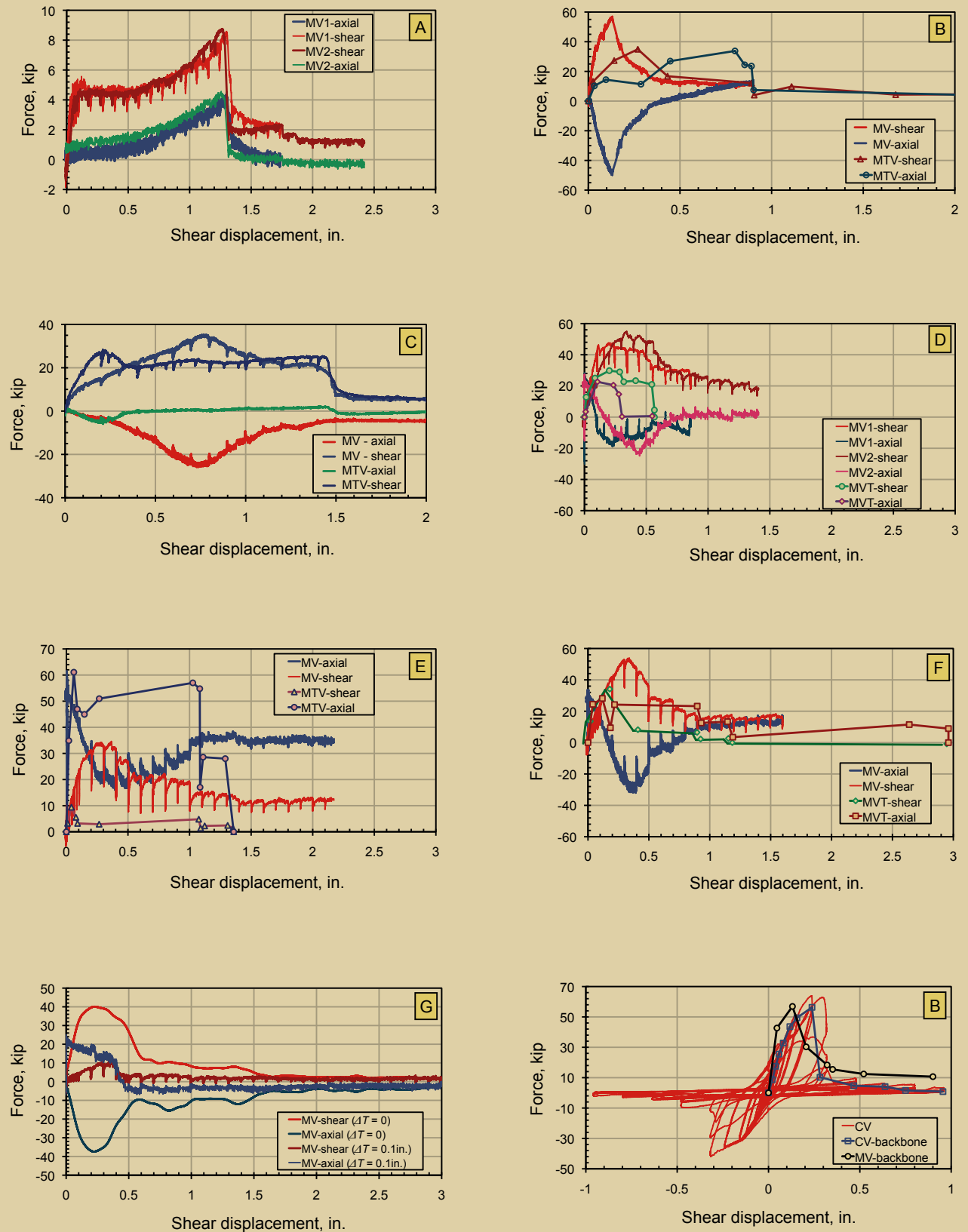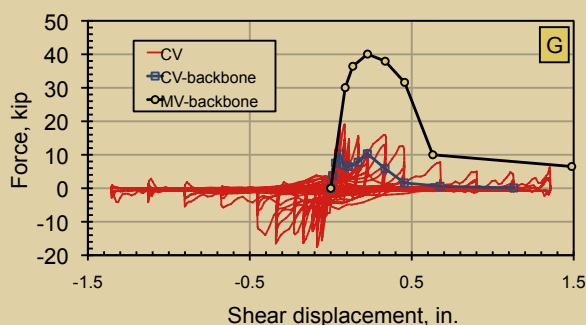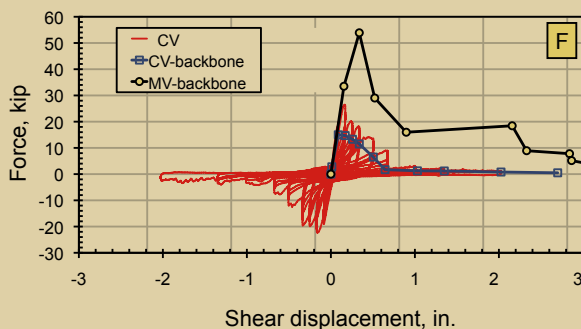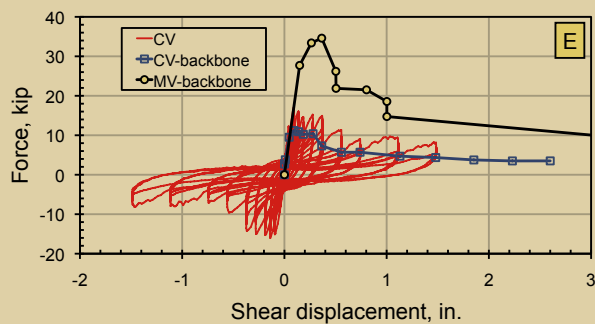
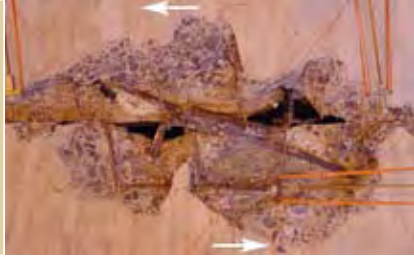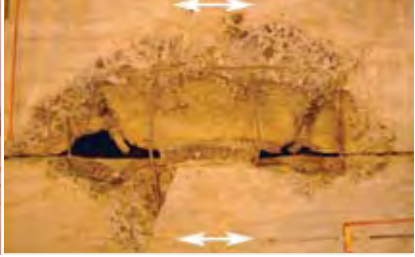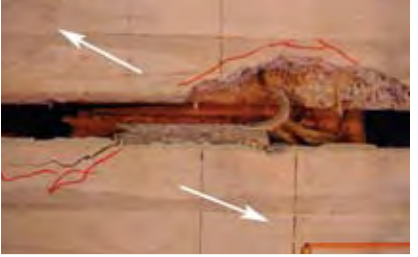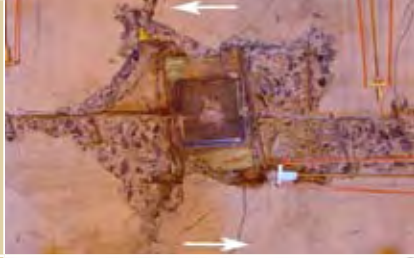**Figure 5.** These graphs summarize the MT, MTV, and CV load-deformation response of each connection. Note: A = untopped hairpin; B = dry chord; C = proprietary connector; CV = cyclic shear; D = stopped hairpin; F = topped cover plate; G = topping with welded-wire reinforcement; MT = monotonic tension; MTV = monotonic tension with shear. $\varDelta T$ = axial joint opening maintained. 1 in. = 25.4 mm; 1 kip = 4.448 kN.

Chart D — Force, kip (vertical axis: -60 to 60) vs Shear displacement, in. (horizontal axis: -3 to 3). Legend: CV, MV-backbone, CV-backbone.

Chart E — Force, kip (vertical axis: -20 to 40) vs Shear displacement, in. (horizontal axis: -2 to 3). Legend: CV, CV-backbone, MV-backbone.

Chart F — Force, kip (vertical axis: -30 to 60) vs Shear displacement, in. (horizontal axis: -3 to 3). Legend: CV, CV-backbone, MV-backbone.

Chart G — Force, kip (vertical axis: -20 to 50) vs Shear displacement, in. (horizontal axis: -1.5 to 1.5). Legend: CV, CV-backbone, MV-backbone.

ed, and eventually the connection was lost by pullout failure of the tension legs at 1.28 in. (32.5 mm) shear.

- Connection B exhibited a high initial stiffness due to bearing of the faceplate and bars on surrounding concrete. A compressive force was generated perpendicular to the joint with an increasing shear deformation. The connection exhibited diagonal cracking in the vicinity of the connector at 0.13 in. (3.3 mm) followed by progressive crushing above the connector, resulting in a significant decrease in bearing areas and degradation in load-carrying capacity. The test was prematurely stopped at a shear deformation of about 1 in. (25 mm). The connector did not fail at this point and most likely would have supported larger deformation at the same load level by means of dowel action.

- The addition of tension in the combined test significantly reduced the shear resistance and delayed the formation of diagonal cracking. Cyclic loading did not considerably affect the ultimate strength over the monotonic response.

- Connection C, the proprietary connection, exhibited local crushing at the leg bend. The shear deformation produced diagonal cracking across the panel at 0.77 in. (19.6 mm), resulting in a decrease of load-carrying capacity. Concrete spalling initiated above the tension leg and eventually led to a pullout at 1.4 in. (35.6 mm) of shear deformation. This tension leg failure could be eliminated by inserting a rod through the holes at the ends of legs.[10]

- In the MVT test, the application of proportional tension demand on this connection prevented diagonal cracking of the concrete. Due to the presence of tension, the compressive force resulting from the shear demand was reduced to a minimal magnitude. This resulted in a 24% decrease in shear strength. The shear deformation capacity, however, was not affected by tensile opening. The connector failed in the same pullout mode as in the MV test.

- Connection D, the field-topped hairpin, exhibited stiff initial response. This can be attributed to the contribution of the topping. A moderate amount of compressive force, 24.5 kip (109 kN), was generated across the joint as the shear deformation demand increased. Diagonal cracking occurred in the concrete topping slab at about 0.3 in. (7.6 mm) and was accompanied by fracture of the WWR at the joint over 0.3 in. to 0.5 in. (12.7 mm) of shear deformation. The connection response returned to an untopped connector embedded in the mid-depth of the 4-in.-thick (102 mm) panel after the topping WWR fractured. Rotation of the slug-weld region occurred with concrete crushing at the interior bar bends. Eventually, the connection

Table 2. Connection condition after testing

Connection	Monotonic shear (MV)	Cyclic shear (CV)	Monotonic shear with tension (MVT)
A		Not conducted	Not conducted
B			
C		Not conducted	
D			
E			
F			
G			Not conducted
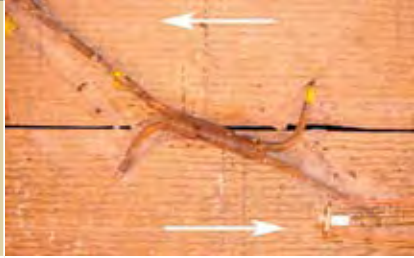
failed by fracture of the tension leg near the root of the slug weld at 2.8 in. (71 mm) shear deformation. Due to the additional restraint provided by the topping slab, the connection compression leg was prevented from buckling and was capable of contributing the same amount of axial resistance as the tension leg. The topped connector produced six times force and two times deformation capacity of the untopped condition.

- Additional tension demand decreased the force and deformation capacity by about 50% and 10%, respectively, over the pure shear response, resulting in bar fracture near the root of the slug weld at 0.55 in. (14 mm). Cyclic loading on this detail reduced the strength to 75% and deformation capacity to 15% of the monotonic response. The connection was lost under 0.64 in. (16.3 mm) due to bar fracture at the end of the cold bend.

- Connection E, the wet chord, exhibited splitting cracks above the embedded bars perpendicular to the joint under 0.1 in. (2.5 mm) tensile opening, indicative of bond slip. With the tensile opening maintained, the shear deformation produced concrete crushing and WWR fracture in the joint. The crushing propagated, resulting in a decrease of bar bearing area and load-carrying capacity. The connector, however, did not fail at this point. A moderate amount of capacity was maintained over a large deformation due to occurrence of a dowel mechanism. Cyclic loading resulted in earlier degradation of the concrete around the mild-steel reinforcement. This produced a rapid loss in bar bearing area and a 70% reduction in shear strength.

- Connection F, the topped cover plate, exhibited diagonal cracking in both topping and precast concrete panels accompanied by WWR fracture at 0.34 in. (8.6 mm) of shear deformation. This was followed by rotation of the cover plate and progressive concrete crushing in the joint, resulting in a decrease of load-carrying capacity. The connection was lost by anchorage bar fracture at the root of bar-to-plate welds. A moderate amount of compressive force was observed during the test.

- The presence of proportional tension produced additional rotation of the connector slug region, resulting in unequal tension demands on anchorage legs. The force and deformation capacity was reduced to 60% of the pure-shear load case. The connector failed by fracture of two diagonally opposite tension legs at about 0.9 in. to 1.1 in. (23 mm to 28 mm) shear deformation. Cyclic loading of this detail reduced the strength and deformation capacity to about 30% of the MV response due to loss of WWR and anchorage bars at a lower deformation level.

- Connection G exhibited diagonal cracks in the topping followed by WWR fracture at 0.23 in. (5.8 mm) of shear deformation when the tensile opening was maintained at zero. With a tensile opening less than 0.1 in., however, the topping failed by WWR fracture without any concrete damage observed. The 0.1 in. (2.5 mm) joint opening yielded the WWR prior to application of shear demands, thus compromising the capacity by 75% without opening. Cyclic loading produced WWR fracture at 0.45 in. (12.7 mm), resulting in a 30% decrease in strength and deformation capacity from that of the monotonic test.
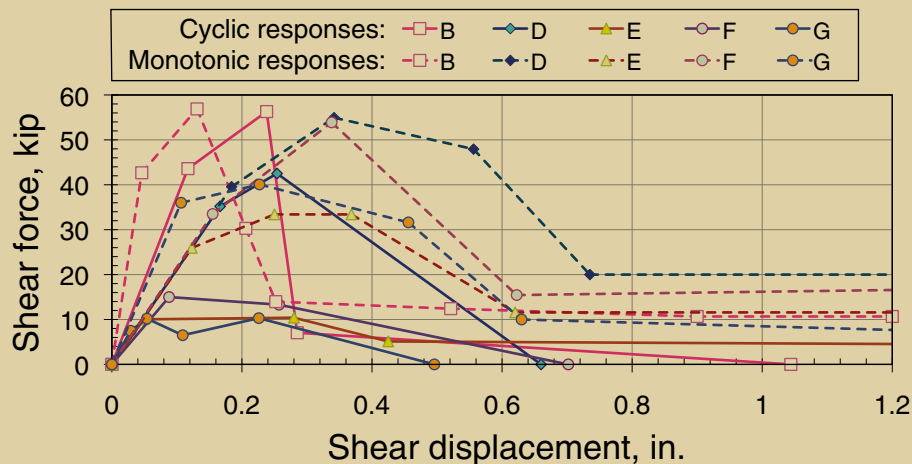

Figure 6. This graph compares monotonic and cyclic shear responses. Note: 1 in. = 25.4 mm; 1 kip = 4.448 kN.
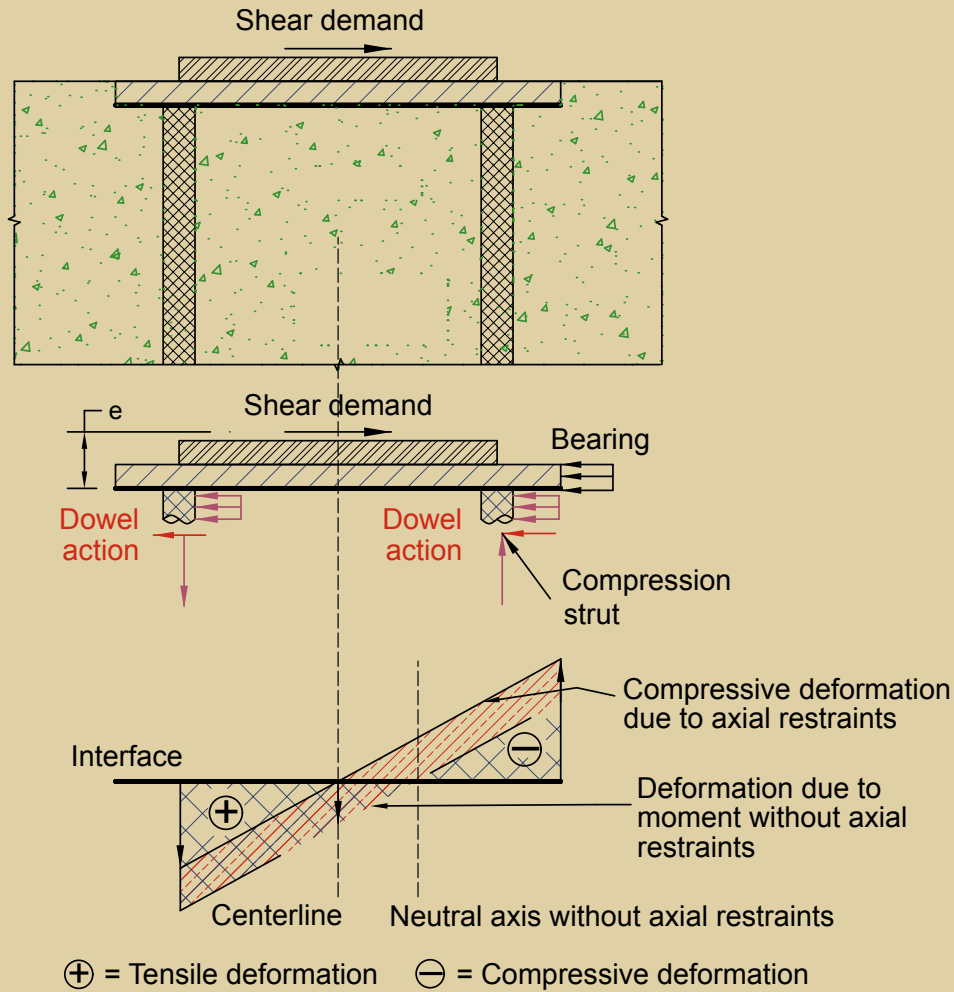
Figure 7. This free-body diagram shows the interface of the precast concrete connection.

Cyclic load effects on shear Cyclic shear tests were conducted on pretopped chord B, topped hairpin D, topped chord E, topped cover plate F, and the topping G. **Figure 6** presents comparisons of the cyclic and monotonic response as simplified shear backbones using the method shown in Fig. 4. The tested connections produced initial shear stiffness over a range from 170 kip/in. to 260 kip/in. (29,800 kN/m to 45,500 kN/m) with the lowest stiffness provided by the topped cover plate F and the highest provided by the pretopped chord B. With the exception of the pretopped chord B, the majority of connections did not exhibit a considerable stiffness reduction due to cyclic loading.

Cyclic loading of the topped connections altered their failure mode and reduced strength and deformation capacity (Fig. 6). WWR fractured earlier in the cyclic tests, achieving about 30% of the monotonic deformation. This can be attributed to low cycle fatigue of the cold-rolled WWR material. Once the WWR fractured, cyclic loading promoted concrete crushing and spalling around the embedded connector, resulting in rapid degradation in load-carrying capacity (Fig. 5). Welded connections D and F failed by bar fracture near the root of the slug weld much earlier than the monotonic test, resulting in brittle response with low ductility.

Influence of axial deformation on shear resistance The application of shear with axial deformation restrained results in the formation of elevated compression across connectors B, C, D, F, and G. These demands produced a combined failure of the connector and the concrete surrounding it. Brittle diagonal cracking and crushing of the concrete initiated first, followed by fracture of the anchorage bars. The reason for these failure modes can be understood by looking at the mechanisms involved in resisting shear. In particular, these mechanisms include bearing of the faceplate and anchorage legs on the concrete and dowel action of the anchorage bars.

Application of shear deformation along the joint produces flexural and compression demands at the connection interface (**Fig. 7**). The moment demand can be attributed to the eccentricity between the center of the connection and the anchorage to the concrete. The moment is resisted through tension provided by the anchorage bar on one side and compression provided by bearing on the concrete on the other. Tensile stiffness of the anchorage bar is relatively small compared with the compressive stiffness of the concrete region. As a consequence, the neutral axis is located close to the compression region under the moment demand. If the joint were free to open and close, the interface would be subjected to an opening deformation based on strain compatibility. The restraint used in the test, however, prevented this motion, and high compression forces approximately equal to the yield axial strength of the connector were developed.

As a result of the bearing and compression on the connector interface, a compression strut formed in the concrete. An increase of shear demand increased the stress in the concrete compression strut until the tension strength perpendicular to the strut was exceeded. A two-dimensional, nonlinear finite-element model (FEM) of the connection demonstrated this mechanism (**Fig. 8** and **9**). The bearing action was active in the front portion of the bar close to the joint, resulting in a high concentration of compressive stress in the concrete (Fig. 8). As the shear deformation exceeded 0.025 in. (0.64 mm), the local bearing stress approached the concrete compressive strength. As a result, the crushing mode of failure initiated at the interface between the interior bar and the concrete (Fig. 9). This mechanism formed in a number of the connection specimens (B, C, D, F, and G). A similar situation would exist in a diaphragm system when the connection is located in the compression zone of the floor diaphragm or when the diaphragm is constrained by a stiff lateral system. It is also likely that for these cases, shear deformation may redistribute to more flexible regions of the diaphragm.

When the connection is in tension or when the concrete bearing mechanism is lost, shear resistance is provided by the dowel action of the anchorage bars. Combined shear and tension deformation at a ratio of 2.0 were conducted on the pretopped chord B. For this connection, the interface shear contribution was significantly reduced due to loss of compression bearing between the concrete and the connector faceplate. The addition of tensile deformation demand generated a tensile force across the joint. Combined loads resulted in unequal tension demands on two anchorage bars (**Fig. 10**). For the connections studied, the presence of concurrent tension resulted in a 58% to 75% decrease in shear resistance.

To minimize the formation of elevated compression forces, debonding and padding can be used. The FEM of the stud-weld connection B was verified with the experimen-
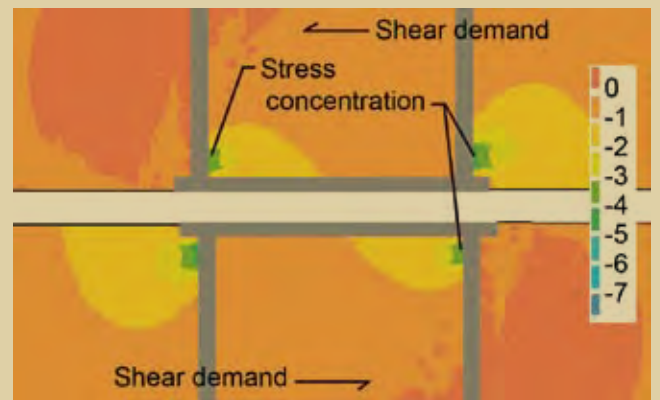

Figure 8. This stress contour is for a double-tee connection at 0.025 in. (0.04 mm) of shear deformation. Note: Scale is in ksi. 1 ksi = 6.89 MPa.
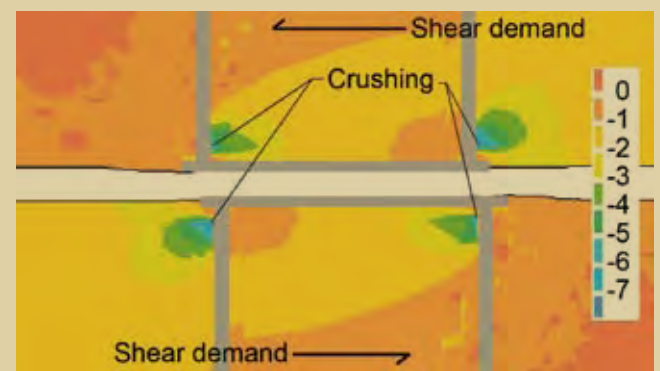

Figure 9. This stress contour is for a double-tee connection at 0.045 in. (1.1 mm) of shear deformation. Note: Scale is in ksi. 1 ksi = 6.89 MPa.

tal data (**Fig. 11**). To illustrate the effect of bar isolation on the shear resistance, a $1/4$-in.-wide (6.4 mm) gap was used along a 4 in. (100 mm) debonded length. Figure 11 compares the load-deformation response with the conventional connection. The debonded chord provided a flexible shear response up to the shear deformation equal to double isolated thickness, which is 0.5 in. (12.7 mm). The use of isolation resulted in a 92% reduction in the shear strength and compression force while increasing the deforma-
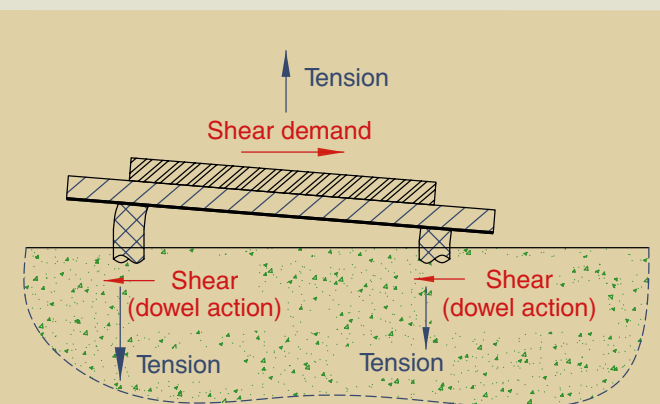

Figure 10. This drawing shows the load demands from combined shear with tension.
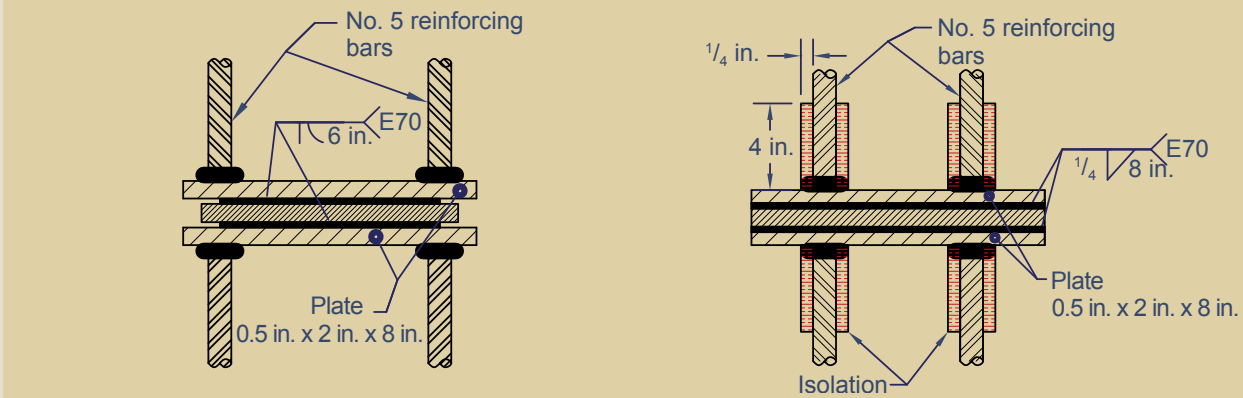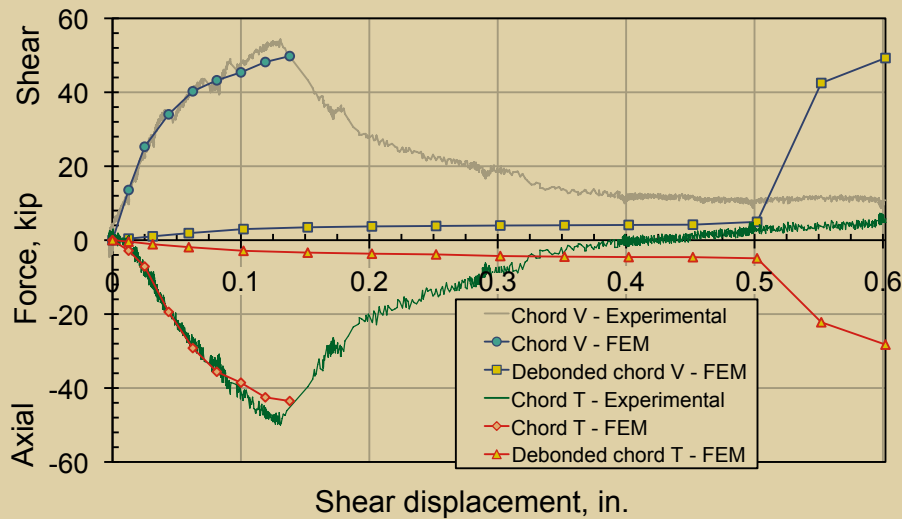
Figure 11. This graph compares the shear response of experimental and FEM results. Note: FEM = finite-element model; T = axial force; V = shear force. 1 in. = 25.4 mm; 1 kip = 4.448 kN.

tion capacity by four times over the conventional chord response. This is attributed to flexible dowel action of the bar within the gap. The interface mechanism previously developed between the anchorage bar and the concrete was not developed due to lack of contact within this deformation range. Without a concentration of compressive stress built up at the connector-to-concrete interfaces, crushing and cracking can be alleviated.

Shear design strength

To predict the diaphragm response during earthquake events, the diaphragm connection capacity must be known. In current design practice, the shear strength of connections is computed based on the truss analogy in *PCI Design Handbook*[20] section 3.8.1.2 or the shear-friction model in *PCI Design Handbook* section 4.3.6 and the American Concrete Institute's *Building Code Requirements for Structural Concrete (ACI 318-05) and Commentary (ACI 318R-05)*[21] section 11.7. The truss analogy

estimates the shear capacity of splayed-leg connectors based on the assumption that the connector leg acts in axial tension and compression to resist shear. For connectors with legs perpendicular to the joint or reinforcements spanning across the joint, the shear resistance can be computed from the shear-friction model. In accordance with ACI 318-05 Eq. (11-25), the capacity is determined from a shear-friction factor μ based on the interface and the assumption that the anchorage legs have yielded.[21]

The experimental results (Fig. 5) indicate that the shear strength increases if concrete shear friction is present. This would occur for the case of a topped system with minimal opening. For connectors B and F, consisting of welded plates, plate bearing on the concrete resulted in local concrete crushing failure at an initial loading stage. Because the bearing failure is brittle and unreliable, the bearing strength is neglected in calculating the nominal resistance.

Table 3. Connector nominal capacity

Connector	Nominal capacity		Measured capacity, kip
	Formulation	kip	
A: hairpin	$f_y A_s \cos 45°$ (tension leg only)	9.3	8.7
B: chord	$f_y A_s \mu$ ($\mu = 0.7$)	29.3	56.9
C: proprietary	$f_y A_s \cos 45°$	17.2	35.9
D: topped hairpin	$f_y 2A_s \cos 45° + f_{wy} A_{ws} \mu$ ($\mu = 0.6$)	30.4	51.3
E: topped chord	$(f_y A_s + f_{wy} A_{ws})\mu$ ($\mu = 0.6$)	37.0	33.8
F: topped cover plate	$f_y A_s \mu_1 + f_{wy} A_{ws} \mu_2$ ($\mu_1 = 0.7, \mu_2 = 0.6$)	27.6	53.9
G: WWR topping ($\Delta T = 0.1$ in.)	$f_{wy} A_{ws} \mu$ ($\mu = 0.6$)	11.8	11.0
G: WWR topping ($\Delta T = 0$)	$f_{wy} A_{ws} \mu$ ($\mu = 1.4$)	27.6	40.1

Note: WWR = welded-wire reinforcement. A_s = cross-sectional area of one anchorage leg of the connection; A_{ws} = total cross-sectional area of WWR crossing the joint; f_{wy} = WWR yield strength; f_y = the yield strength of the anchorage leg; ΔT = joint opening; μ = shear-friction factor; μ_1 = shear-friction factor for cover plate bars; μ_2 = shear-friction factor for welded-wire reinforcement. 1 in. = 25.4 mm; 1 kip = 4.448 kN.

Table 3 provides the nominal estimated capacity for each connection. The nominal strength is computed using the mill-certified material properties in **Table 4** to provide correlation with the experimental results. For connector design, the standard assumptions for yield should be used along with an appropriate strength-reduction factor. The following terminology is used in the formulations presented:

- cross-sectional area of one anchorage leg of the connection A_s

- yield strength of the anchorage leg f_y

- total cross-sectional area of WWR crossing the joint A_{ws}

- WWR yield strength f_{wy}

The concept behind each formulation is discussed with respect to the connector configuration.

Splayed-leg connectors

Shear capacity of the splayed-leg connector (proprietary and topped hairpin) is computed by taking the component of both the compression and tension anchorage legs in the direction of shear. For an untopped hairpin connector embedded in the 2-in.-thick (50 mm) panel, however, shear resistance should be computed with the tension leg only. Shear strength is calculated from the horizontal component. The monotonic shear test on the untopped detail showed that the compression leg buckles and provides minimal strength due to a rapid loss of concrete bearing surface on the exterior bend.

Perpendicular-leg connectors

Shear capacity of reinforcement perpendicular to the joint (pretopped chord connector, cover-plate connector, and WWR) is obtained by multiplying the shear-friction factor by the yield strength of the reinforcement crossing the joint. Determination of which shear-friction factor to use is

Table 4. Material properties

Materials	Yield strength, ksi	Tensile strength, ksi
ASTM A706 steel no. 4 bar	65.8	91.4
ASTM A706 steel no. 5 bar	67.6	95.6
ASTM A304 stainless steel	51.5	96.9
W2.9 wire	85.0	103.3

Sources: Data from American Society for Testing and Materials (ASTM) Subcommittee A01.05, "Standard Specification for Low-Alloy Steel Deformed and Plain Bars for Concrete Reinforcement," ASTM A706/A706M–08a (West Conshohocken, PA: ASTM), and ASTM Subcommittee A01.15, "Standard Specification for Carbon and Alloy Steel Bars Subject to End-Quench Hardenability Requirements," ASTM A304–05e2 (West Conshohocken, PA: ASTM). Note: No. 4 = 13M; no. 5 = 16M. 1 ksi = 6.89 MPa.
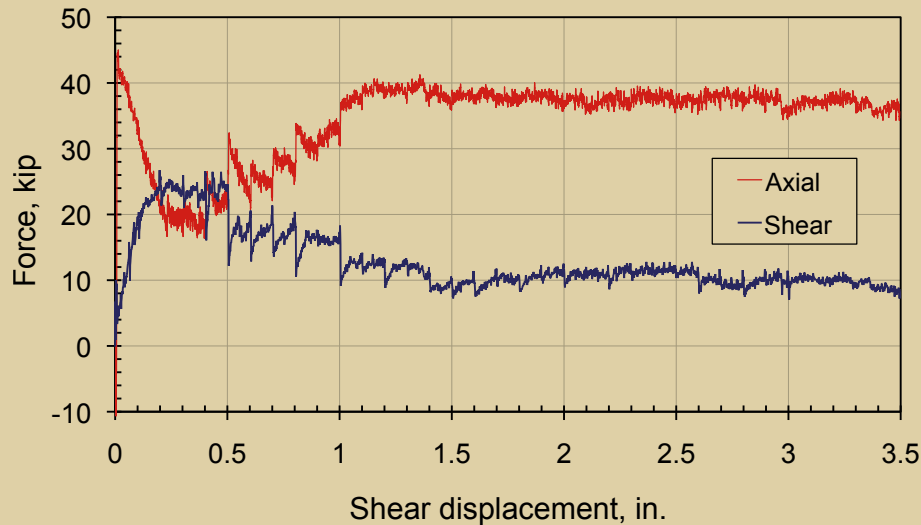
Figure 12. This graph shows the response of two no. 5 (16M) anchorage bars in connection E. Note: 1 in. = 25.4 mm; 1 kip = 4.448 kN.

dependent on the interface condition. Pretopped chord and cover-plate connections can be categorized as "concrete anchored to as-rolled structural steel by reinforcing bars," according to ACI 318-05 section 11.7.4.3, or "concrete to steel" per the *PCI Design Handbook*, and use a factor equal to 0.7. Precracked topping slabs can be categorized as "concrete placed against hardened concrete not intentionally roughened." Therefore, a shear-friction factor equal to 0.6 is used.[20,21] Uncracked topping slabs are fabricated under the condition of "concrete placed monolithically," and a high shear-friction factor of 1.4 is used.[20,21] In a parking structure, however, most topping slabs are typically cracked above the double-tee panel joints under the service load due to shrinkage and thermal effects. To be conservative, the joint can be assumed to be cracked in the calculation. This approach by using appropriate shear-friction factors is capable of providing a good estimate of the shear capacity of similar connections in previous tests.[13]

Topped connections

Topped connections consist of embedded connectors and WWR in the topping across the joint. In computing the nominal capacity of the topped connectors, the assumption was made that the WWR and connector both achieve their yield strengths at the same time and the capacity of WWR is assumed to be additive with that of the underlying connector.

Table 1 compares the nominal capacity with the measured capacity by means of strength ratios. The average strength ratio of connections B, C, D, F, and closed-joint G ($\Delta_t = 0$) was greater than 1.0 under the pure shear deformation demand. Shear loading on these connections generated high axial restraining force, which in turn remarkably elevated the shear-friction capacity along the joint. The shear-friction factor used in the estimation does not account for this overstrengthening due to compression, thus the method provides a conservative estimate. The shear ratio of connection G with 0.1 joint opening ($\Delta_t = 0.1$) was about 1.0. Thus, the shear-friction factor proposed by ACI 318-05 gives an accurate estimate.

As a result, connections B, C, D, F, and G met the proposed nominal capacity equations presented. Connections A and E did not meet the nominal capacity equations proposed. The formulation used for connection A, the untopped hairpin, assumes that the entire anchorage legs are adequately embedded inside the concrete panel. Achieving this condition in a 2-in.-thick (50 mm) panel is difficult, resulting in minimal bar embedment and premature pullout of the tension leg.

Table 5. Comparison for shear strength of two no. 5 bars in connection E

	Shear displacement, in.	Tension demand, kip	Measured capacity, kip	Calculated capacity, kip
At peak	0.365	20.0	23.5	21.3
Post peak	>3.5	37.4	11.2	11.0

Note: 1 kip = 4.448 kN.

Ductile topping option

Temperature and shrinkage WWR — Ductile joint WWR ladder — Field-placed topping

0.25 in.

Side elevation

Precast concrete flange

Temperature and shrinkage WWR

Lap — Ductile joint WWR ladder

Traditional, nonductile, cold-rolled temperature and shrinkage WWR
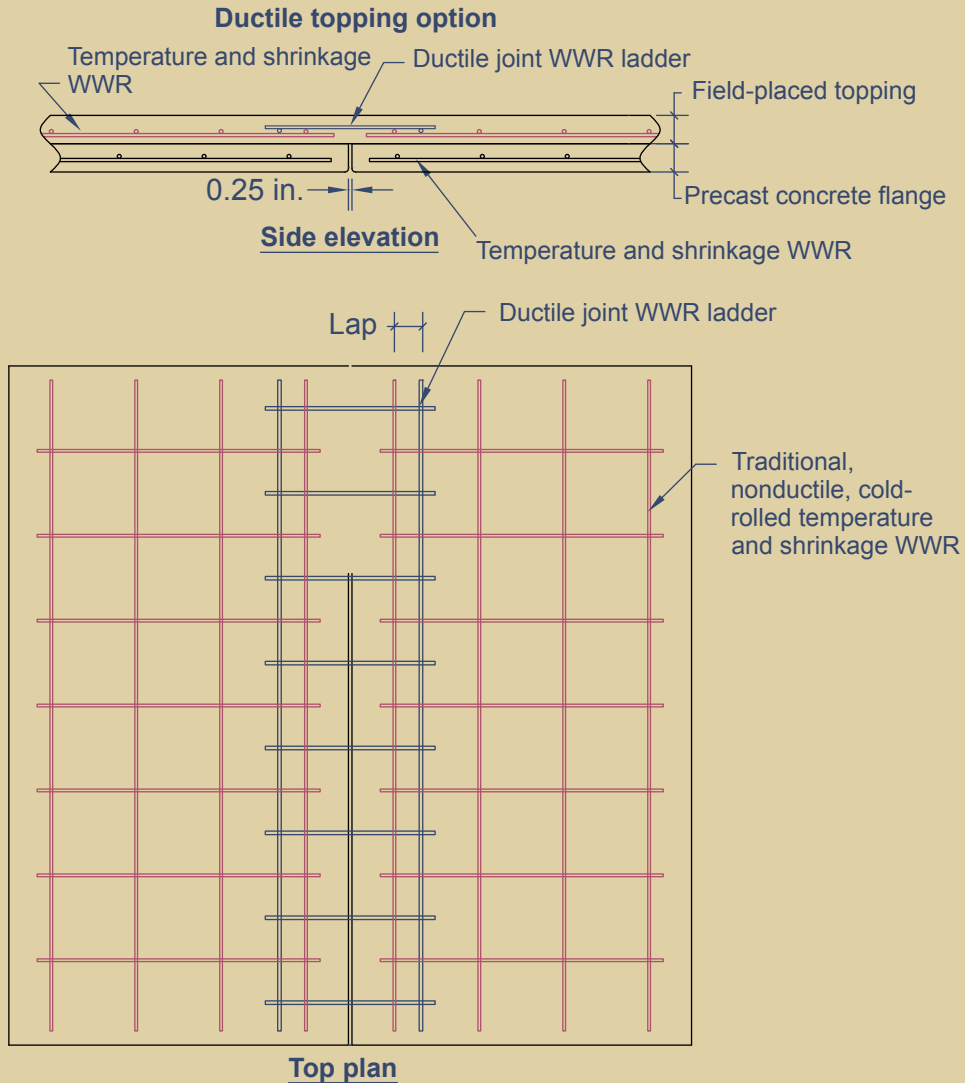
Top plan

Figure 13. This drawing illustrates the ductile topping details. Note: WWR = welded-wire reinforcement. 1 in. = 25.4 mm.

A similar condition existed for the pour-strip connection E. Because the pour-strip bars were embedded in a 2-in.-thick topping slab, shear produced compression failure of the topping as opposed to shear friction across the interface. Shear resistance was decreased by this failure mode and degraded remarkably under cyclic conditions. Consequently, the shear capacity of the pour strip should only be accounted for if an adequate embedment is provided.

Shear-strength reduction for continuous reinforcement under tension The relationship between shear and tensile strength of continuous reinforcements across the joint can be estimated with the Von Mises plastic yield criterion in Eq. (1).

$$\sigma^2 + 3\tau^2 = f_y^2 \qquad (1)$$

where

σ = tensile stress

τ = shear stress

f_y = yield strength of the steel material

In the absence of tension ($\sigma = 0$), the shear stress achieves the maximum value of $f_y / \sqrt{3}$ or $0.6f_y$. Thus, shear capacity of a connection without tension can be estimated as presented in Table 3. As observed in shear tests, shear strength is compromised by concurrent tension force. This

sensitivity can be accounted for by rearranging Eq. (1) into Eq. (2).

$$\tau = \frac{1}{\sqrt{3}}\sqrt{f_y^2 - \sigma^2} = 0.6\sqrt{f_y^2 - \sigma^2} \qquad (2)$$

Assuming $\sigma = \alpha f_y$ the nominal shear strength V_n is predicted as shown in Eq. (3).

$$V_n = \tau A = 0.6\sqrt{1 - \alpha^2}\left(f_y A\right) \qquad (3)$$

where

A = cross-sectional area of bar crossing joint

α = ratio of tensile stress to yield strength of connection material = σ/f_y

Thus, the codified shear-strength factor of 0.6 is reduced by $\sqrt{1 - \alpha^2}$ due to the addition of tension stress σ.

The response of connection E under monotonic shear is presented in **Fig. 12**. As shown, the connection is subjected to a varying amount of tension force. Given the applied tension demand, the shear strength of the connection can be computed using Eq. (3). As presented in **Table 5**, this method provides a 91% estimate of the measured peak shear capacity V_b and a 99% estimate of the residual capacity V_c. The shear-strength factor of $0.6\sqrt{1 - \alpha^2}$ is recommended for cases in which concurrent tension demands exist.

Connection detailing recommendations

The majority of double-tee connections tested exhibited stiff but brittle shear response with high capacity and low deformability due to a concrete crushing mode of failure. Some connections produced ductile response; however, the resistance was limited. To enhance the deformation capacity, connections should be detailed to reduce undesirable concrete failure and transfer the demand from concrete into the connector:

- Untopped hairpin connections should be properly anchored in the mid-depth of the panel to ensure sufficient embedment depth. This installation can prevent leg-pullout failure and allow for yield mechanism developed in the diagonal tension legs in two adjacent panels. Conventional hairpins accumulate residual stresses due to the cold-bending operation by which they are made. The residual stresses result in premature fracture of the bar at the bend under cyclic-load reversals. To improve the connection deformability, the bar should be bent through a hot-work process.

- Recent research suggests that pretopped chord connections should be mechanically debonded behind the faceplate to allow for tensile ductility.[22] To enhance the shear flexibility and deformability, foams can be used at the end of the faceplate and over the debonded length of anchorage legs.

- Topped connections exhibited a brittle shear response due to limited deformability of WWR. Currently, WWR manufactured in the United States is cold rolled from ASTM A510[23] Grade 1018 or 1022 steel. The cold-working process results in significant residual strain, which greatly reduces the deformation capacity of the material. As a consequence, the deformability of WWR is much lower than that of the connectors used within the precast concrete panel. To address this, a ladder WWR detail is recommended for use along the joint (**Fig. 13**). This detail provides predictable axial and shear capacity and a significant increase in deformability over conventional WWR. Due to the larger diameter of wire used, the ladder can be fabricated from material not subjected to the cold-rolling process. This provides a topping connection that maintains deformation capacity comparable with that of the embedded connectors used in the precast concrete panels.

Conclusion

The experimental research program examined the shear performance of seven connections representative of typical pretopped and topped connections commonly used in current U.S. precast concrete construction. From the test observations and discussions presented, the following conclusions are drawn:

- Shear response of precast concrete double-tee connections is often governed by connector bearings on surrounding concrete. The shear capacity is provided by interface shear mechanism and anchorage bar dowel action.

- Cyclic loading can alter the failure mechanism and often reduces the shear strength and deformation capacity. The majority of connections fail by a steel fracture mode at a smaller deformation level than the monotonic test. The initial shear stiffness, however, is not affected.

- For pretopped chord B, proprietary connector C, topped hairpin D, topped cover plate F, and uncracked topping G, shear deformation coupled with axial restraint resulted in a high shear resistance and high axial compression force. The compression force was a result of equilibrium and compatibility at the connection interface.

- Tension was generated across the joint when untopped hairpin A, topped chord E, and precracked topping G were subjected to shear demands. The presence of tension reduced the shear strength to that of a dowel action mechanism.

- The shear strength of double-tee connections can be conservatively estimated by relying on shear friction or a modified-truss analogy. Formulations are presented and are shown to compare well with experimental results.

- The hairpin connection is capable of resisting moderate shear forces over a large deformation range. Topped hairpin connections provide a greater resistance and deformability than untopped hairpin connections provide because of additional restraint provided by the topping. To ensure the desirable truss mechanism, the connector should be properly anchored at the mid-depth of the panel.

- The stud-weld connection provides stiff shear response with high resistance and low ductility. To improve shear flexibility, a debonded length can be used to allow shear compliance of the anchorage bars.

- The use of 2-in.-thick (50 mm) topping on a 2 in. precast concrete section with ¼ in. (6.4 mm) of roughness and WWR spaced at 10 in. (254 mm) provides stiff and brittle shear response over a 0.5 in. (12.7 mm) deformation. Due to the brittle material property of cold-drawn WWR, current topping detailing is not appropriate for high seismic design. A recommended topping ladder fabricated from smooth, hot-rolled wire is presented.

References

1. Wood, S., J. Stanton, and N. Hawkins. 2000. New Seismic Design Provisions for Diaphragms in Precast Concrete Parking Structures. *PCI Journal*, V. 45, No. 1 (January–February): pp. 50–65.

2. Fleischman, R., C. Naito, J. Restrepo, R. Sause, and S. K. Ghosh. 2005. Precast Diaphragm Seismic Design Methodology (DSDM) Project, Part 1: Design Philosophy and Research Approach. *PCI Journal*, V. 50, No. 5 (September–October): pp. 68–83.

3. Fleischman, R. B., C. Naito, J. Restrepo, R. Sause, S. K. Ghosh, G. Wan, M. Schoettler, and L. Cao. 2005. Precast Diaphragm Seismic Design Methodology (DSDM) Project, Part 2: Research Program. *PCI Journal*, V. 50, No. 6 (November–December): pp. 14–31.

4. Fleischman, R. B., R. Sause, S. Pessiki, and A. B. Rhodes. 1998. Seismic Behavior of Precast Parking Structure Diaphragms. *PCI Journal*, V. 43, No. 1 (January–February): pp. 38–53.

5. Venuti, William J. 1970. Diaphragm Shear Connectors between Flanges of Prestressed Concrete T-Beams. *PCI Journal*, V. 15, No. 1 (February): pp. 67–78.

6. Aswad, A. 1977. Comprehensive Report on Precast and Prestressed Connections Testing Program. Research report, Stanley Structures Inc., Denver, CO.

7. Spencer, R. 1986. Earthquake Resistant Connections for Low Rise Precast Concrete Buildings. Seminar on Precast Concrete Construction in Seismic Zones, V. 1, NSF/Japan Society for the Promotion of Science.

8. Kallros, M. K. 1987. An Experimental Investigation of the Behavior of Connections in Thin Precast Concrete Panels under Earthquake Loading. MS thesis, Civil Engineering Department, University of British Columbia, Canada.

9. Pincheira, J. A., M. G. Oliva, and F. I. Kusumo-Rahardjo. 1998. Tests on Double Flange Connectors Subjected to Monotonic and Cyclic Loading. *PCI Journal*, V. 43, No. 3 (May–June): pp. 82–96.

10. Oliva, M. G. 2000. Testing of the JVI Flange Connector for Precast Concrete Double Tee Systems. Structures and Materials Test Laboratory, University of Wisconsin, Madison, WI.

11. Shaikh, A. F., and E. P. Feile. 2002. Testing of JVI Vector Connector. University of Wisconsin, Milwaukee, WI.

12. Wiss, Janney, Elstner Associates Inc. 2002. Dayton/Richmond Flange-to-Flange Connector Tests. Miamisburg, OH.

13. Pincheira, J. A., M. G. Oliva, and W. Zheng. 2005. Behavior of Double-Tee Flange Connectors Subjected to In-Plane Monotonic and Reversed Cyclic Loads. *PCI Journal*, V. 50, No. 6 (November–December): pp. 32–54.

14. Van de Lindt, J. W., and H. A. de Melo e Silva. 2005. Uniform Serviceability Load Limits for Mechanical Flange Connectors. *ASCE Practice Periodical on Structural Design and Construction*, V. 10, No. 1: pp. 34–39.

15. Naito, C., and L. Cao. 2004. Precast Diaphragm Panel Joint Connector Performance. Paper 2722, Proceedings 13th World Conference on Earthquake Engineering, Vancouver, Canada.

16. Cao, L. 2006. Effective Design of Precast Concrete Diaphragm Connections Subjected to In-plane Demands. PhD thesis. Lehigh University, Bethlehem, PA.

17. Naito, C., L. Cao, and W. Peter. 2009. Precast Concrete Double-Tee Connections, Part 1: Tension Behavior. *PCI Journal*, V. 54, No. 1 (Winter): pp. 49–66.

18. Priestley, M. J. N. 1992. The U.S.–PRESSS Program Progress Report. Third Meeting of the U.S.–Japan Joint Technical Coordinating Committee on Precast Seismic Structural Systems (JTCC-PRESSS), San Diego, CA.

19. Building Seismic Safety Council 1997. *NEHRP Guidelines for the Seismic Rehabilitation of Buildings*. Federal Emergency Management Association (FEMA) pub. 273. Washington, DC: FEMA.

20. Industry Handbook Committee. 2004. *PCI Design Handbook: Precast and Prestressed Concrete*. 6th ed. Chicago, IL: PCI.

21. American Concrete Institute (ACI) Committee 318. 2005. *Building Code Requirements for Structural Concrete (ACI 318-05) and Commentary (ACI 318R-05)*. Farmington Hills, MI: ACI.

22. Cao, L., and C. Naito. 2007. Design of Precast Diaphragm Chord Connections for In-Plane Tension Demands. *Journal of Structural Engineering*. V. 133, No. 11 (November): pp. 1627–1635.

23. ASTM Standard A510. 2007. *Standard Specification for General Requirements for Wire Rods and Coarse Round Wire, Carbon Steel*. West Conshohocken, PA: ASTM International.

Notation

A = cross-sectional area of bar crossing joint

A_s = cross-sectional area of one anchorage leg of the connection

A_{ws} = total cross-sectional area of welded-wire reinforcement crossing joint

C_b = coupled axial force at the level of peak shear resistance

f_{wy} = welded-wire-reinforcement yield strength

f_y = yield strength of anchorage leg

K_s = shear stiffness

V_a = shear resistance at point a

V_b = shear resistance at point b

V_c = shear resistance at point c

V_{es} = estimated strength

V_n = nominal shear strength

α = ratio of tensile stress to yield strength of connection material
= σ/f_y

Δ_t = tension deformation

ΔT = joint opening

Δ_v = shear deformation

ΔV_a = shear displacement at point a

ΔV_b = shear displacement at point b

ΔV_c = shear displacement at point c

μ = shear-friction factor

μ_1 = shear-friction factor for cover plate bars

μ_2 = shear-friction factor for welded-wire reinforcement

About the authors

Clay Naito, PhD, P.E., is an associate professor for the Department of Civil and Environmental Engineering at Lehigh University in Bethlehem, Pa.

Liling Cao, PhD, is a senior engineer with Thornton Tomasetti in New York, N.Y.

Synopsis

An experimental study of double-tee, flange-to-flange connections was conducted as part of the PCI/National Science Foundation–funded research effort on the development of a seismic design methodology for precast concrete diaphragms. The research program categorizes the strength and deformation capacity of common double-tee web and chord connectors subjected to in-plane shear or tension loading.

This paper presents the experimental results of floor diaphragm connectors subjected to in-plane shear and in-plane shear with tension deformation. The results are compared with expected capacities. The majority of connections subjected to shear with opening restrained exhibited high compression forces coupled with high shear capacity. The application of tension, however, compromised the shear strength.

The chord connections tested were found to provide high shear resistance over a limited deformation. Web connectors in topped diaphragm systems provided a high initial shear resistance but returned to the untopped response once the topping reinforcement was lost. The topping slab reinforced with welded-wire reinforcement exhibited brittle shear response with high initial stiffness and strength prior to wire fracture. To improve the connection strength and deformability, recommendations on connector detailing are presented.

Keywords

Review policy

Reader comments